Monte Carlo Ground State Energy Approximations for Trapped Boson Systems

Trinity University Department of Physics and Astronomy

20 April 2012

An Undergraduate Thesis Written By: Ethan M. Rudd

Thesis Advisor: Dr. Nirav Mehta _____

Department Chair: Dr. Dennis Ugolini _____

Dr. Kelvin Cheng _____ Dr. Eugene Clark _____

Dr. David Hough _____ Dr. Gordon MacAlpine _____

Dr. Daniel Spiegel _____ Dr. Jennifer Steele _____

Abstract

Diffusion Monte Carlo (DMC) and Green's Function Monte Carlo (GFMC) algorithms were implemented to obtain numerical approximations for the ground state energies of systems of bosons in a harmonic trap potential. Gaussian pairwise particle interactions of the form $V_0 e^{-|r_i - r_j|^2/{r_0}^2}$ were implemented in the DMC code. These results were verified for small values of V_0 via a first-order perturbation theory approximation for which the N-particle matrix element evaluated to $\binom{N}{2} \frac{V_0}{(1+2/{r_0}^2)^{3/2}}$. Details regarding the convergence of the GFMC algorithm are discussed.

Acknowledgements

I would like to thank Dr. Mehta for his invaluable perspicacity, cogent explanations, enthusiasm, and guidance, as well as for providing a great deal of time, patience, and resources which made this project feasible. We are very lucky to have him in the Trinity physics department.

Contents

1 Introduction

Although analytical solutions for the Schrödinger equation are feasible for the hydrogen atom, more complex atomic structures must be approximated numerically. However, integration of the N-body Schrodinger equation is no easy task: while the equation is separable for potentials that are constant in time, matrix diagonalization of the time-independent equation becomes impractical since computational complexity grows exponentially with dimension (c.f. [8]), and quickly exceeds current computational capacity. Therefore, physicists have turned to less conventional methods for solving quantum multi-body problems.

Monte Carlo methods, first implemented during the Manhattan Project, are a class of algorithms which achieve their results through iterated random sampling of one or more random variable distributions. A basic example of a Monte Carlo algorithm involves integration by taking n repeated random samples on a uniform interval $[a, b]$, where a and b are the lower and upper limits of the integral, finding the value of the function in question at each of these points, summing the values, and multiplying the sum by the length of the interval divided by the number of points (cf. [5, p. 171]). As intuition suggests, Monte Carlo methods have better convergence properties than their than their $O(e^N)$ mesh-based counterparts.

In this paper, we shall explore two Monte Carlo algorithms that are commonly used to solve for the ground state energies of N-particle systems. The first algorithm we shall explore will be the Green's Function Monte Carlo algorithm (GFMC) in which the integral time-independent Schrödinger equation is obtained via the exact time-independent Green's function. Monte Carlo integration is then used to iterate this integral equation until convergence to the ground state is obtained, which is guaranteed by the power method for finding eigenvalues. The second algorithm that we shall examine is the Diffusion Monte Carlo (DMC) algorithm, in which the time-dependent Schrödinger equation is written in imaginary time and an approximation to the time-dependent Green's function is used to obtain an iterable integral equation.

1.1 The 3N-dimensional Schrödinger Equation

Let N be the number of particles. The coordinates of each corresponding particle may be represented by $\mathbf{x}_i$, $i = 1, 2, ..., N$. Let $\Phi = \Phi(\mathbf{x}_1, ..., \mathbf{x}_N)$ and V be a function of both the positions

of the particles with respect to an external potential $(\mathbf{x}_1, ..., \mathbf{x}_N)$ and the positions of the particles with respect to each other $(\mathbf{x}_i - \mathbf{x}_j; i \neq j)$. Then, assuming that all particles are of equal mass, m, the Schrödinger equation reads:

$$-\sum_{i=1}^{N} \frac{\hbar^2}{2m} {\nabla_i}^2 \Phi + V\Phi = E\Phi \tag{1}$$

Writing the problem in units where $\frac{\hbar^2}{m} = 1$, and introducing the energy shift ${V_{max}}$[1], the equation reads as,

$$-\nabla^2\Phi(\mathbf{X}) - 2(E_0 - V_{max})\Phi(\mathbf{X}) = -2(V(\mathbf{X}) - V_{max})\Phi(\mathbf{X}), \tag{2}$$

where $\mathbf{X}$ is the $3N$-dimensional vector corresponding to the coordinates of all particles, E_0 is the ground state energy, and Φ is the wavefunction of the N-particle system.

By introducing the variable $k^2 = -2(E_0 - V_{max})$, where k is the wave number, we may write equation (2) in a more revealing form (cf. [7, pp. 103-104]):

$$\left[-\frac{1}{k^2}\nabla^2 + 1\right]\Phi(\mathbf{X}) = \left[\frac{V(\mathbf{X}) - V_{max}}{E_0 - V_{max}}\right]\Phi(\mathbf{X}) \tag{3}$$

Thus, we have a problem of the form:

$$L\Phi(\mathbf{X}) = f(\mathbf{X}), \tag{4}$$

where L is the linear operator $[-\frac{1}{k^2}\nabla^2 + 1]$, and $f(\mathbf{X})$ is the right hand side of equation (3). Now, by definition,

$$LG(\mathbf{X}, \mathbf{Y}) = \delta(\mathbf{Y} - \mathbf{X}), \tag{5}$$

where $G(\mathbf{X}, \mathbf{Y})$ is the Green's function of L, δ is the Dirac delta function, and $\mathbf{Y}$ is an arbitrary position vector in our coordinate system. Since $f(\mathbf{X}) = \int \delta(\mathbf{Y} - \mathbf{X}) f(\mathbf{Y}) d\mathbf{Y}$, by the definition of

[1]This may be required to make all energies negative, which is necessary for a closed form of the Green's function (cf. [7, p. 103]).

the Dirac delta, we may rewrite the right hand side of equation (4) as

$$f(\mathbf{X}) = \int \delta(\mathbf{Y} - \mathbf{X}) f(\mathbf{Y}) d\mathbf{Y} = \int LG(\mathbf{X}, \mathbf{Y}) f(\mathbf{Y}) dy. \tag{6}$$

Hence,

$$L\Phi(\mathbf{X}) = \int LG(\mathbf{X}, \mathbf{Y}) f(\mathbf{Y}) d\mathbf{Y}. \tag{7}$$

Since L is an operator acting on $\mathbf{X}$, we may pull it out of the integral. We may now remove L from both sides of the equation. Now,

$$\Phi(\mathbf{X}) = \int G(\mathbf{X}, \mathbf{Y}) f(\mathbf{Y}) d\mathbf{Y}. \tag{8}$$

Re-substituting for f yields the integral equation (cf. [7, pp. 103-104])

$$\Phi(\mathbf{X}) = \int G(\mathbf{X}, \mathbf{Y}) \left[\frac{V(\mathbf{Y}) - V_{max}}{E_0 - V_{max}} \right] \Phi(\mathbf{Y}) d\mathbf{Y}. \tag{9}$$

By using the appropriate Green's function (cf. [8],[7, pp. 103-104]),

$$G(\mathbf{X}, \mathbf{Y}) = \frac{1}{(2\pi)^{(\nu+1)}} \mathbf{r}^{\nu} K_{\nu}(\mathbf{r}) \tag{10}$$

where $\mathbf{r} = k \mid \mathbf{X} - \mathbf{Y} \mid$, we have an integral form of the Schrödinger equation which we will iterate to solve for ground state energy.

1.2 Importance Sampling

Importance sampling is used as a means of decreasing variance, and, in the case of the GFMC algorithm, decreasing convergence time by changing both the sampling algorithm and the function to be sampled. Consider the example given in the introduction of integrating a function $f(x)$ over

an interval using a uniform distribution. If we instead let $h(x) = \frac{f(x)}{g(x)}$, and re-write the integral as

$$\int_a^b f(x)dx = \int_a^b h(x)g(x)dx, \tag{11}$$

we can sample at random[2] N times from $g(x)$, evaluate $h(x)$ at each of these sample points, sum these N values, and multiply by $\frac{b-a}{N}$ to obtain an integral with lower variance and faster convergence, provided the "guiding function" $g(x)$ is well chosen (it should mimic $f(x)$).[3] We can implement importance sampling in our integral equation by re-writing equation (9) as (cf. [7, p. 104])

$$\Psi(\mathbf{X})\Phi(\mathbf{X}) = \int \frac{\Psi(\mathbf{X})}{\Psi(\mathbf{Y})} G(\mathbf{Y},\mathbf{X}) \left[\frac{V(\mathbf{Y}) - V_{max}}{E_0 - V_{max}}\right] \Phi(\mathbf{Y})\Psi(\mathbf{Y})d\mathbf{Y}. \tag{12}$$

In equation (12), Ψ is the trial wavefunction which we choose prior to iteration as an initialization for Φ. Thus, before iterating, Φ is equal to Ψ. However, Ψ does not change over the course of iterating, whereas Φ evolves to the ground state wavefunction. We shall elaborate on this presently.

2 The GFMC Algorithm

2.1 Overview

The GFMC algorithm is a stochastic variational algorithm which iterates equation (12) for some trial wavefunction, until convergence to the ground state is obtained. First, we will consider what the algorithm effectively does, then we will discuss implementation.

The general idea is to start out with an initial trial wavefunction, represented by a state vector of potential particle configurations, each with probability given by the trial wavefunction evaluated at that configuration. For simplicity, momentarily ignore importance sampling and consider equation (9). The integral can therefore be interpreted as a state vector being multiplied by a stochastic matrix, $\mathbf{P}$, with the ijth element representing the transition probability from current state i to state j. The new state vector obtained can be thought of as a position representation of the new wavefunction (cf. [5, pp. 175-177,210-211]). Because each iteration is independent of the last, we

[2] This entails obtaining values along the uniform interval $[0, 1]$, via a seeded deterministic algorithm then transforming these values via an inverse transformation so that they correspond to the appropriate distribution function (cf. [11, pp. 287-298]).

[3] cf. [5, p. 172]

can think of the sequence of iterations as a Markov chain (cf. [11, p. 408]) ultimately converging to the ground state.

Convergence to the ground state is guaranteed by the Power method (cf. [2, pp. 576-579]) (or Inverse Power method [2, pp. 583-585], depending on one's interpretation) as follows:

We can represent the 'stochastic matrix' in equation (9) as a constant, A, times an operator, $\mathbf{S}$, which is the inverse operator of the Hamiltonian (cf. [7, p. 79]). We can then rewrite equation (9) as

$$\Phi_{n+1} = A\mathbf{S}\Phi_n. \tag{13}$$

Now, expand Φ_0 in terms of its eigenfunctions $\Phi^{(k)}$, where the C_k are constants:

$$\Phi_0 = \sum_k C_k \Phi^{(k)}. \tag{14}$$

Since $\mathbf{S}$ is the inverse of the Hamiltonian, if $E^{(k)}$ is the eigenvalue of the Hamiltonian corresponding to $\Phi^{(k)}$, then $\mathbf{S}\Phi^{(k)} = \frac{\Phi^{(k)}}{E^{(k)}}$ (cf. [8]). Now, we iterate as follows:

$$\Phi_1 = A\mathbf{S}\sum_k C_k \Phi^{(k)} = \sum_k C_k \Phi^{(k)} \frac{A}{E^{(k)}}, \tag{15}$$

$$\Phi_2 = A^2\mathbf{S}\mathbf{S}\sum_k C_k \Phi^{(k)} = \sum_k C_k \Phi^{(k)} \left(\frac{A}{E^{(k)}}\right)^2, \tag{16}$$

$$\ldots$$

$$\Phi_n = A^n\mathbf{S}^n\sum_k C_k \Phi^{(k)} = \sum_k C_k \Phi^{(k)} \left(\frac{A}{E^{(k)}}\right)^n. \tag{17}$$

The ratio $\frac{A}{E^{(k)}}$ has greatest magnitude for the smallest magnitude $E^{(k)}$, which we will denote $E^{(0)}$, corresponding to the lowest magnitude energy (the ground state energy). As $n \to \infty$, $\Phi_n \to \Phi^{(0)}$ times a constant. In other words, after enough[4] iterations, the state vector converges to that of the ground state.

[4]For the systems considered in this thesis "enough" was found to be $O(1000)$. For further discussion of convergence see section 3.2.

2.2 Implementation

While matrix multiplication is one way to interpret the algorithm, implementation in this manner engenders the problem of computational complexity. Instead of attempting to deal with every conceivable state, a Monte Carlo implementation allows us to examine an ensemble of a few relevant configurations, where each configuration is known as a 'walker'. We implement the iteration of the integral equation in two parts: a 'branching part' and a 'diffusion part'.[5]

2.2.1 Branching

The branching term of the integral equation (equation (9)) consists of (cf.[7, 105-107])

$$\left[\frac{V(\mathbf{Y}) - V_{max}}{E_0 - V_{max}}\right]. \tag{18}$$

In the algorithm, we append copies of walkers to the ensemble according to this term, where the integer value of the sum of the term and a random number sampled from the uniform interval $[0, 1]$ is the number of clones to append. If this integer is equal to zero, we remove the walker from the ensemble. We can make physical sense of this as follows: walkers with potential energy less than E_0 are reproduced, whereas walkers with potential energy greater than E_0 are removed. This is easy to visualize in the case of a 1-dimensional harmonic oscillator potential. Walkers in the well below E_0, (i.e. near the ground state) thrive, whereas walkers outside of the well, or in the well at energies much higher than the ground state die. In short, we can think of the branching part of the algorithm as a filter which restricts our ensemble of walkers to relevant configurations. Note that we do not know the ground state energy ahead of time. In this case, E_0 is an educated guess for the ground state energy, commonly referred to as the "trial energy". We show that E_0 converges to the true ground state energy after many iterations (see equation(21)).

2.2.2 Diffusion

The diffusion term of the integral equation (equation (9)) is (cf.[7, 105-107])

$$G(\mathbf{Y}, \mathbf{X})\Phi(\mathbf{Y})d\mathbf{Y}. \tag{19}$$

[5]These implementations come from diffusion and rate equations obtained in the Diffusion Monte Carlo (DMC) algorithm (cf. [7, pp. 88-92]). Incidentally, GFMC is a time integrated form of DMC.

This term dictates the movement of the walkers from configuration $\mathbf{Y}$ to $\mathbf{X}$. The diffusion part of the algorithm is a modification of the Metropolis method (cf. [10]), in which a step in a random direction on the 3N-dimensional unit hypersphere is attempted, with radius given by sampling the Green's function at random. The state change is accepted under the following conditions (cf. [1]).

1. If the ratio $\frac{\Psi(\mathbf{X})}{\Psi(\mathbf{Y})}$ is greater than or equal to 1, then the change is accepted.
2. If $\frac{\Psi(\mathbf{X})}{\Psi(\mathbf{Y})} < 1$, a random number is sampled from the uniform distribution [0,1]. If the random number is less than $\frac{\Psi(\mathbf{X})}{\Psi(\mathbf{Y})}$, the change is accepted. Otherwise the change is rejected and the walker is removed from the ensemble.

2.2.3 Importance Sampling Revisited

In section 1.2, we introduced an equation which implements importance sampling by introducing the term $\frac{\Psi(\mathbf{X})}{\Psi(\mathbf{Y})}$ into the integral equation. In our algorithm, we can implement this by assigning weight $W = \frac{\Psi(\mathbf{X})}{\Psi(\mathbf{Y})}$ to each walker in the diffusion part of the algorithm, provided that the step is accepted (cf. [1]). In the next iteration of the branching, we multiply this weight by the term in (18). For a given walker, the branching factor[6], MB, becomes

$$MB = \text{int}(W\left[\frac{V(\mathbf{Y}) - V_{max}}{E_0 - V_{max}}\right] + U[0,1]), \tag{20}$$

where $U([0,1])$ is a random number from the uniform interval [0,1], W is the weight, and int denotes that we are taking the floor integer value of the quantity in parentheses.

Intuitively, we expect our the algorithm to have faster convergence with importance sampling, because higher transition probability ratios are weighted more heavily.

2.3 Obtaining the Ground State Energy

So far, we have talked about the algorithm's convergence properties, but have not explained how to extract the ground state energy. Fortunately, this is an easy task. Although it is not readily apparent, we can obtain an estimate of the ground state energy at the nth iteration by taking the average of the local energies of all the walkers (cf. [1, p. 99]). This is feasible since by definition,

[6] i.e. the number of copies of a walker to make.

the expectation value of the local energy is the mean of all the local energies (cf. equation (22)). The proof goes like[7]

$$\langle E_{loc} \rangle = \frac{\int \Phi(\mathbf{X})\Psi(\mathbf{X})\frac{\hat{H}\Psi(\mathbf{X})}{\Psi(\mathbf{X})}d\mathbf{X}}{\int \Phi(\mathbf{X})\Psi(\mathbf{X})d\mathbf{X}} = \frac{\int \Phi(\mathbf{X})\hat{H}\Psi(\mathbf{X})d\mathbf{X}}{\int \Phi(\mathbf{X})\Psi(\mathbf{X})d\mathbf{X}} = E_0 \frac{\int \Phi(\mathbf{X})\Psi(\mathbf{X})d\mathbf{X}}{\int \Phi(\mathbf{X})\Psi(\mathbf{X})d\mathbf{X}} = E_0, \qquad (21)$$

where E_0 is the ground state energy. This relationship applies to both GFMC and DMC algorithms.

2.4 Initialization

The algorithm begins by initializing an ensemble of walkers for a given number of particles, with positions, a trial wavefunction, a potential, and a local energy, each depending on position. While theoretically, any normalized trial wavefunction should work for the algorithm, good guesses (i.e. guesses that are close to the actual wave function) are more feasible computationally, as far as attaining stability in number of walkers and convergence rate. Local energy depends on Ψ as

$$E_{loc} = \frac{\hat{H}\Psi(\mathbf{X})}{\Psi(\mathbf{X})}, \qquad (22)$$

where $\mathbf{X}$ is a $3N$-dimensional position vector. We must also seed the algorithm with a guess for E_0, which we may change several iterations into the algorithm to be the average of the local energy over all walkers, in order to accelerate convergence. An energy shift of V_{max} is required if we are dealing with positive potentials, so as to make all energies negative. If we are dealing with potentials that are unbounded from above, as in the case of the quantum harmonic oscillator, we can still obtain a valid approximation by choosing V_{max} such that $V_{max} \gg E_0$ because practically zero walkers will sample $E_{loc} > V_{max}$.

Although initialization may vary depending on the system in question, we use a fairly general technique of sampling a unit-vector from the $3N$-dimensional hypersphere, then assigning a random magnitude, sampled from whatever distribution best suits the problem. While obtaining a randomly oriented unit vector is a straightforward task for one, two, or three dimensions, it is not so simple in $3N$-dimensions. We will therefore use a technique elaborated on in the next section.

[7]Since $\hat{H}$ is a hermitian operator, it can legitimately act on Φ from the right.

2.5 Sampling Techniques

2.5.1 Obtaining a Unit $3N$-dimensional Vector

First we randomly sample the Gaussian, $e^{-{\zeta_1}^2-{\zeta_1}^2-{\zeta_2}^2-\ldots-{\zeta_{3N}}^2}$, $3N$ times to obtain a vector $(\zeta_1, \zeta_2, ..., \zeta_{3N})$. Our $3N$-dimensional unit vector, $(\alpha_1, \alpha_2, ..., \alpha_{3N})$, has components defined by the normalization of this vector (cf. [8]),

$$\alpha_i = \zeta_i \left(\sum_j \zeta_j^2 \right)^{-\frac{1}{2}} . \tag{23}$$

A quick visual verification of this sampling technique is shown in Figure 1. N was set to 1 and points were plotted over 1000 iterations. As probability dictates, the resulting plot traces out the unit sphere.

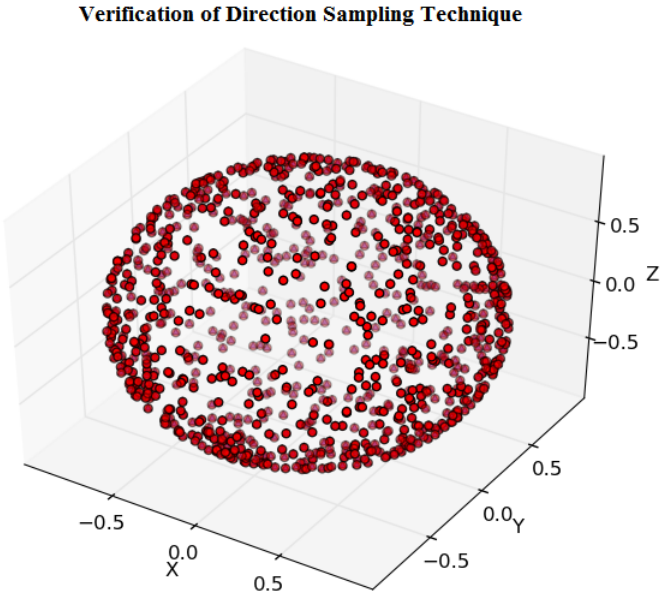

Figure 1: Direction Sampling Verification

2.5.2 Sampling the Green's Function

The diffusion part of the algorithm relies on sampling the Green's function (equation (10)) at random to determine the magnitude of the attempted step, R. We do so using the following technique (cf. [8]):

First, we sample a uniform distribution [0,1] 3N+1 times, to get the random numbers, $\zeta_0, \zeta_1, \zeta_2, ..., \zeta_{3N}$. We then take the negative natural logarithm of the product of the last 3N of these random numbers and set it equal to u, and call v the square root of one minus the first of these random numbers, raised to the power of $2/(3N-1)$. We therefore have

$$u = -ln(\zeta_1 \zeta_2 ... \zeta_{3N}) \tag{24}$$

and

$$v = (1 - {\zeta_0}^{2/(3N-1)})^{\frac{1}{2}}. \tag{25}$$

The product, uv, is then equal to the magnitude hyper-radius, R, and is thus equivalent to a random sample of the Green's function.

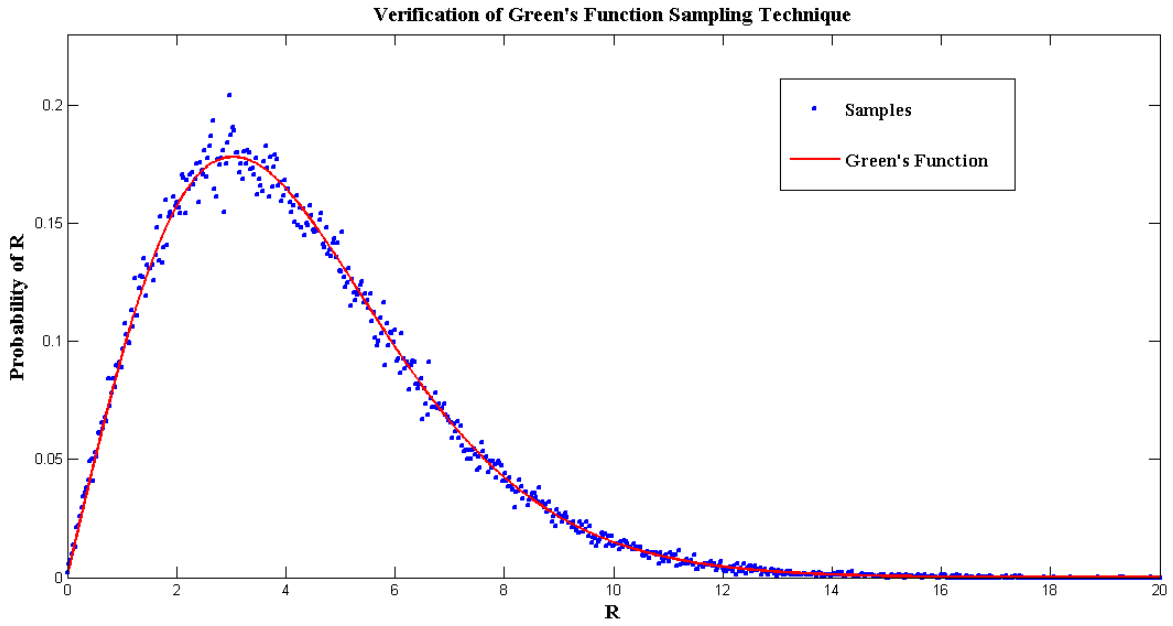

Figure 2: Green's Function Sampling Verification

This sampling technique was verified by plotting 1,000 normalized 'bins' of 100,000 samples

along with the actual Green's function (equation 10), shown in red. The results are shown in Figure 2. The fact that the Green's function is closely approximated by the plot of the bins indicates that the sampling technique is working correctly.

3 GFMC Results and Discussion

3.1 Summary

The algorithm was tested for quantum harmonic oscillator potentials with one, two, three, and four non-interacting particles. Convergence was also obtained for Gaussian trial wavefunctions of different shape and scale parameters than those of the actual wavefunctions. Although average energies seemed to move in the proper direction for all wavefunctions tested, walker population explosions made convergence verification impossible when the trial wavefunction differed from the actual wavefunction by shape and scale parameters of unit order. Certain techniques were used to attempt to accelerate convergence and keep walker growth in check. Although these techniques were successful to some degree, the problem of extreme walker population arresting convergence persisted for many trial wavefunctions. Despite the shortcomings of our current implementation, we include a description of the technique and a summary of our results so that the code can be improved in the future.

3.2 Determining Convergence

Because the GFMC algorithm is a stochastic algorithm, we cannot simply assign a tolerance as one can with deterministic convergent algorithms (e.g., root finding methods). Thus what determines convergence is somewhat of an open question. If the result is known, as is the case with quantum harmonic oscillator systems, then we can compare the approximated energies directly to the actual result. The question then becomes how to determine the quality of convergence. Because a given step is more likely than a series of steps to be an outlier, a less error-prone approach is to take the average energy and standard deviation over many walker-steps, then compute standard error. One must be careful, however, not to measure these quantities too early, as this will produce inaccurate results. There is no general unambiguous way to determine when to start taking averages, as it depends on how long the algorithm runs, the system in question, initial conditions, and

the stochastic nature of the algorithm. A general rule of thumb is that asymptotic average walker energy as a function of step number indicates convergence, since the Power method guarantees that GFMC will converge exponentially. Therefore, averages should only be taken once sufficient constancy in energy as a function of step number has been established. "Sufficient constancy", however, is subjective to the accuracy desired. Accuracy may be assessed via standard error.[8] For a given number of steps, lower standard error indicates better convergence.

Our methodology for taking averages involved running the algorithm for a given set of parameters, examining the results after a given number of iterations, determining when convergence was attained via the aforementioned methods, and using this step number as baseline to begin taking averages for ground-state energy determination.

3.3 Accelerating Convergence and Walker Population Control

Given a trial wavefunction, a system converges faster when the estimate of the ground state energy is near the actual ground state energy. If the actual ground state energy is not known, however, then a way to accelerate convergence is to set the trial E_0 to the average walker energy for the next iteration, once the algorithm has had a chance to stabilize. This affects the branching part of the algorithm, and will cause fewer walkers which branch out of control to be created.

3.4 Results for One, Two, and Three Particles in a QHO Potential

We shall now present results, selectively chosen to illustrate some of the more pertinent aforementioned points.

Solutions to the $3N$-dimensional isotropic harmonic potential are easily obtained (neglecting particle interactions), because the Schrödinger equation for this system is separable into $3N$ one-dimensional systems. The full ground state wavefunction is

$$\psi_0(\mathbf{X}) = \left(\frac{m\omega}{\pi\hbar}\right)^{3N/4} e^{-\sum_{i=1}^{3N}({X_i}^2)/2}, \tag{26}$$

[8] The central limit theorem guarantees that we may use standard error for GFMC uncertainty estimation (cf. [5, pp. 161-163]).

where X_i is the ith component of $\mathbf{X}$, and the potential energy is

$$V = \frac{1}{2} m\omega^2 |\mathbf{X}|^2. \tag{27}$$

To simplify things for the following test cases, we express everything in units mass m =1 and angular frequency $\omega = 1$, so that the actual wavefunction becomes

$$\psi_0(\mathbf{X}) = \left(\frac{1}{\pi}\right)^{3N/4} e^{-\sum_{i=1}^{3N}({X_i}^2)/2}, \tag{28}$$

and the potential becomes

$$V = \frac{1}{2} |\mathbf{X}|^2. \tag{29}$$

As one can see, the actual wavefunction is a 3N-dimensional Gaussian. A natural choice for a similar yet incorrect trial wavefunction is a Gaussian of different width. Thus, for our trial wavefunction, we choose

$$\Psi(\mathbf{X}) = \left(\frac{1}{\pi}\right)^{3N/4} \left(\frac{1}{X_{0t}}\right)^{3N/2} e^{-\sum_{i=1}^{3N}({X_i}^2)/2{X_{0t}}^2}. \tag{30}$$

where X_{0t} is the standard deviation parameter of the Gaussian, not equal to one.

The local energy for this trial wavefunction is

$$E_{loc} = \frac{\hat{H}\Psi(\mathbf{X})}{\Psi(\mathbf{X})} = \frac{1}{2}\left(\sum_{i=1}^{3N} {X_i}^2\right)\left(1 - \frac{1}{{X_{0t}}^4}\right) + \frac{3N}{2{X_{0t}}^2}. \tag{31}$$

Because the ground state energy of a one-dimensional quantum harmonic oscillator is $\frac{1}{2}\hbar\omega$, the ground state energy of a $3N$-dimensional harmonic oscillator is $\frac{3N}{2}\hbar\omega$, or $\frac{3N}{2}$ in our units, with $\omega = 1$ and $\hbar = 1$.

We initialize the locations of the walkers via the technique discussed in Section 2.4, with radii randomly sampled from a Gaussian distribution centered at 0 with standard deviation $\sigma = 1/\sqrt{2}$.

3.4.1 One Particle

Figure 3 illustrates the convergence of the algorithm for one particle in three dimensions. One particle average energy is shown in blue. Actual ground state energy is shown in red. Ground state

trial energy was initialized at $E_0 = 1.7$. The initial number of walkers was 1000. X_{0t} was set to 1.5. The maximum ensemble size was 90,000. The average walker energy taken from step 2350 to 2450 (1957239 walkers×steps) was 1.4986 ± 0.0003. Convergence to within 1% of the correct trial energy of 1.5 occurred after approximately 1000 steps.

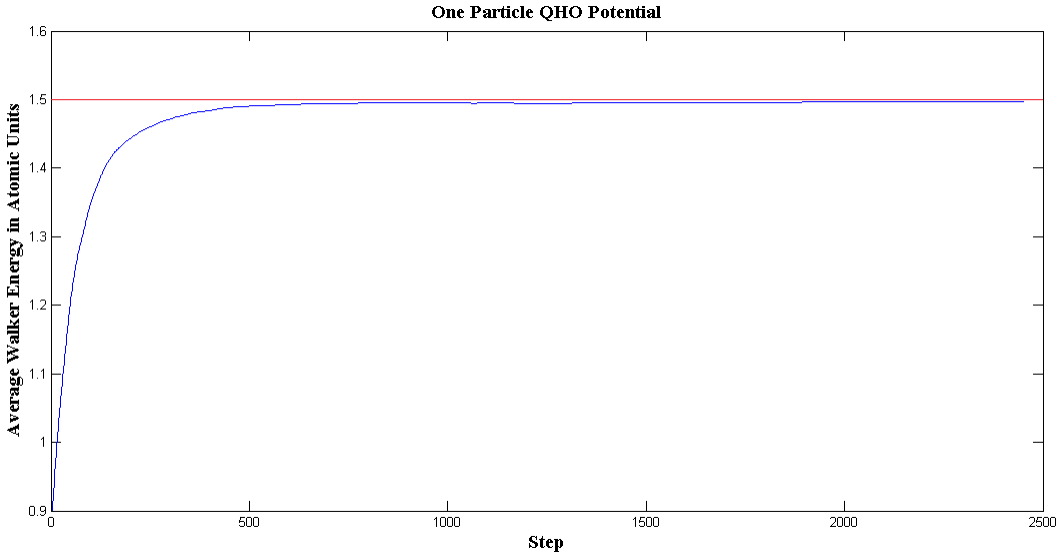

Figure 3: One particle average energy vs. step number.

Walker growth as a function of step number is shown in Figure 4. We notice that the walker growth rate decreases considerably after step 500. This is because the initial estimate for the ground state energy was 1.7, but was changed to the average energy of the ensemble after 500 steps. As one can see, this attempt to keep the number of walkers in check was marginally successful. Running the algorithm without this change caused the ensemble to exceed the maximum allotted ensemble size of 90,000 before the 1000th step.

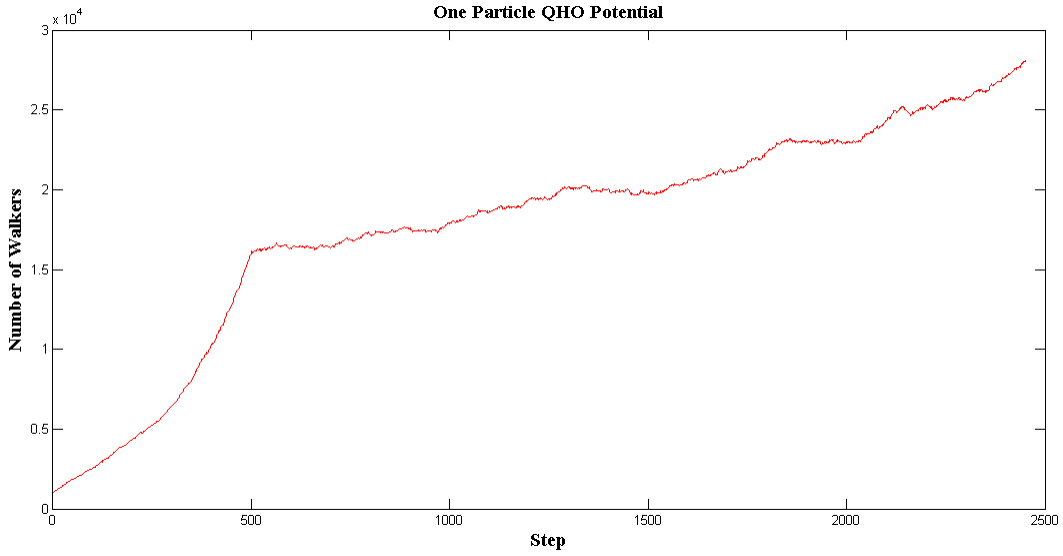

Figure 4: Number of walkers as a function of step number.

3.4.2 Two Particles

Figures 5 and 6 show convergence and walker growth for the two particle case. As one can see, walker growth is again checked at step 500 by the change of ground state energy guess from 3.2 to the average local energy of all the walkers. Although iterating the integral equation theoretically gives exponential convergence, we notice small bumps in the plot in Figure 5. These occur because of the stochastic nature of the algorithm, and the fact that we cannot represent all possible configurations simultaneously.

In Figure 5 two particle average energy is shown in blue. Actual ground state energy is shown in red. Ground state trial energy was initialized at $E_0 = 3.2$. X_{0t} was set to 1.5. The initial ensemble size was 1,000. The maximum ensemble size was 90,000. Average walker energy from step 800 to 890 (7,764,967 walkers$\times$steps) was 2.9853 ± 0.0003. After step 890, the maximum ensemble size was exceeded.

Number of walkers as a function of step are shown in Figure 6. Note the effects of changing the estimate of the ground state energy to the average walker energy at step 500.

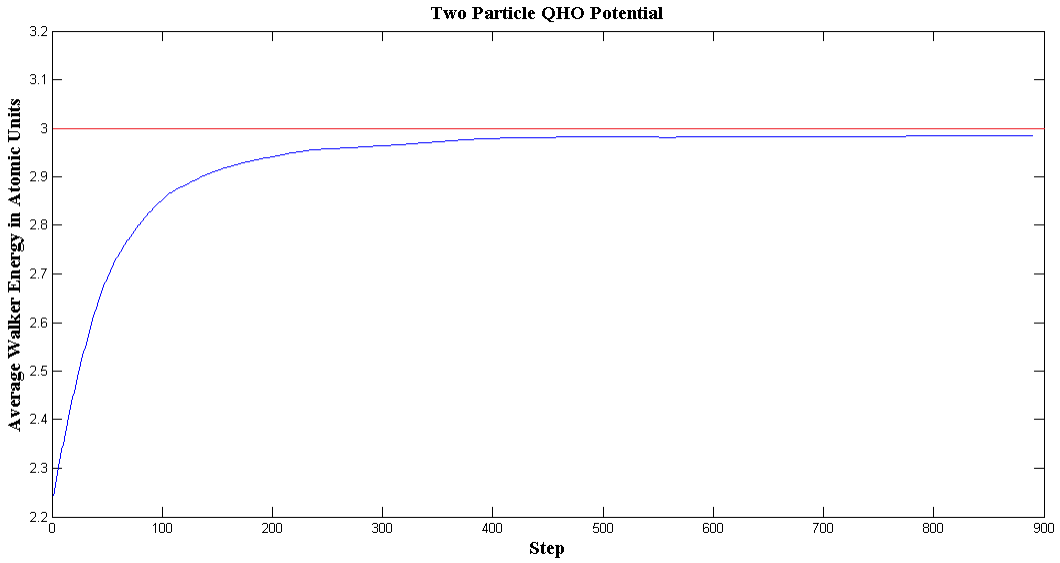

Figure 5: Two particle average energy vs. step number.

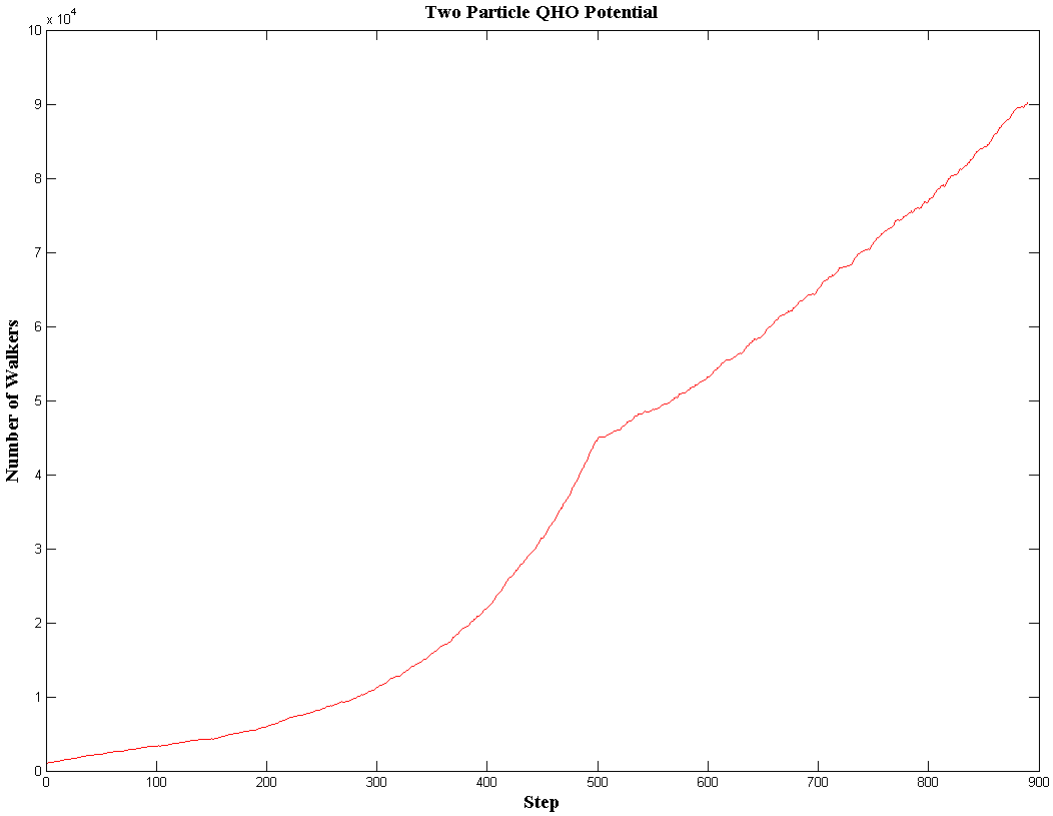

Figure 6: Number of walkers as a function of step number.

3.4.3 Three Particles

Although convergence can be seen for the three particle case, the maximum ensemble size of 90,000 was exceeded before the 500th step in the run shown in Figures 7 and 8. Toggling initial conditions allowed for a 2500 step trial, although the ensemble size was first changed to 200,000.

In Figure 7, three particle average energy is shown in blue. Actual ground state energy is shown in red. Ground state trial energy was initialized at $E_0 = 4.7$. X_{0t} was set to 1.2. The initial ensemble size was 1,000. Maximum ensemble size was 90,000. Average walker energy from step 400 to 433 (2,429,407 walkers×steps) was 4.4734 ± 0.0006. After step 433, the maximum ensemble size was exceeded.

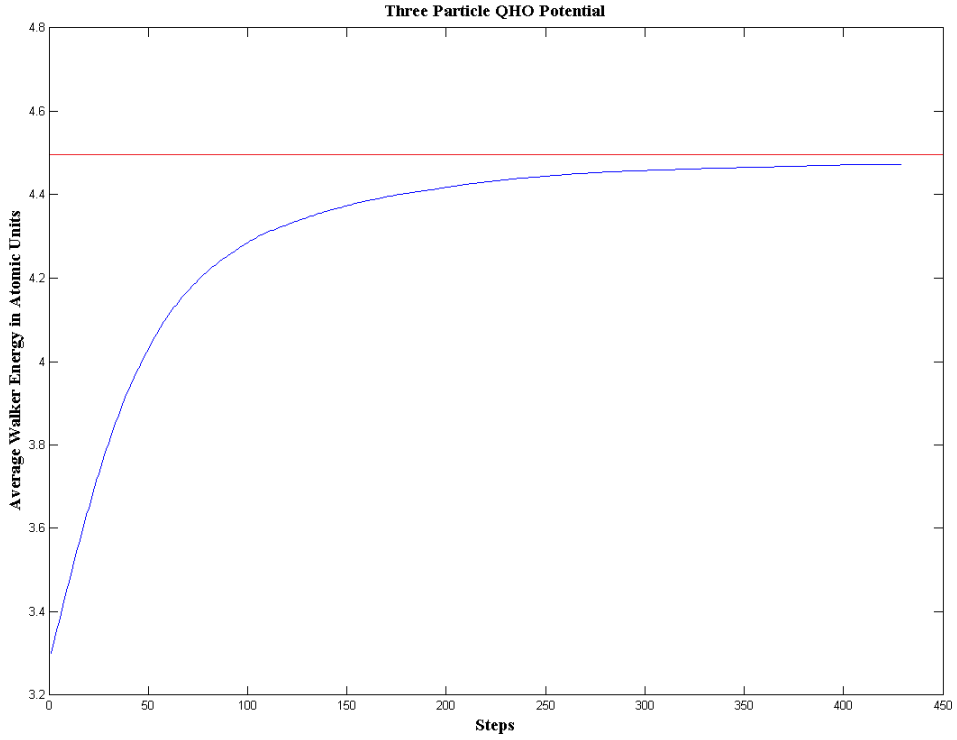

Figure 7: Three particle average energy vs. step number.

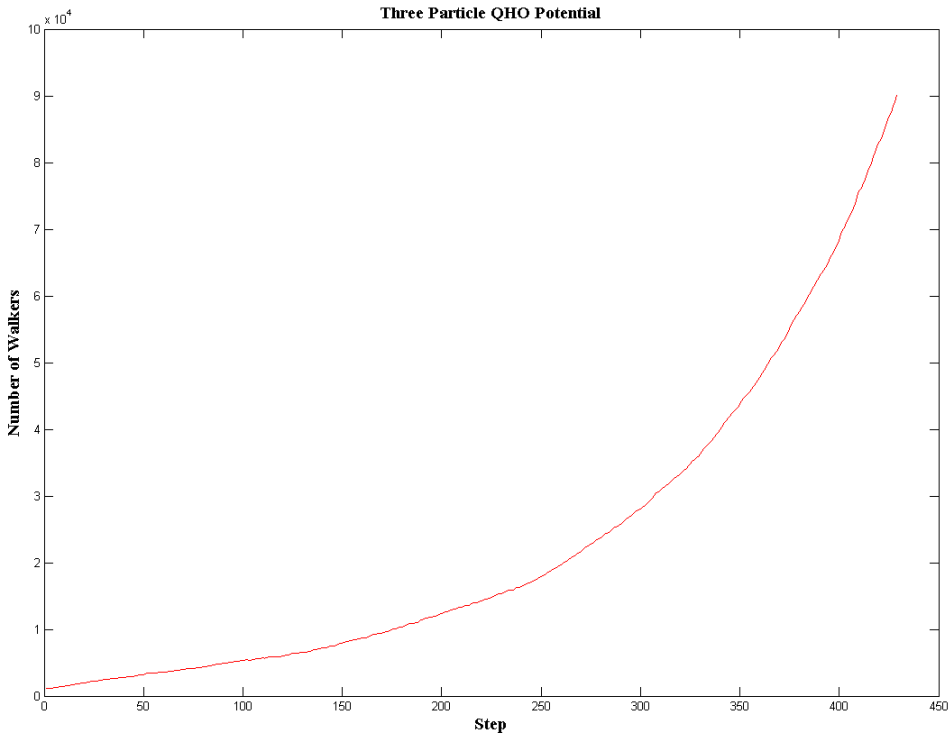

Figure 8: Number of walkers as a function of step number.

3.5 Discussion

From our experimental trials, it is apparent that walker growth is a problem, even when the trial wavefunction is similar to the actual wavefunction. Although increasing the maximum ensemble size allows the algorithm to run longer, this does not solve the problem at hand of exponential walker growth, because it buys only a few more iterations before computer RAM limitations become a problem. Although certain choices of trial E_0 limit walker growth, walker population was nonetheless a problem for any choice we attempted, save for the actual ground state energy.

Additionally, walker growth becomes more of a problem with increases in dimensionality. This makes sense because for higher dimensions there are more degrees of freedom, and therefore more states. As one can see, even with a better trial wavefunction, and similar initial conditions to the previous one and two particle systems, the three particle system exceeded the ensemble size before the 500th step.

A characteristic of the algorithm which bears mentioning is that for the trials depicted in the plots, the direction of convergence is opposite of what one might intuit from the variational principle.

The reason for this is quite straightforward: the intuition is faulty. Quantum Monte Carlo is an algorithmic technique in which the distribution of walkers converges to the ground state. Until convergence is reached, however, the walker distribution does not necessarily satisfy the Rayleigh-Ritz criterion[9]. Technically, the initial walker layout need not even be normalizable. Moreover, walkers represent particle configurations; *not* particles. The probabilty distribution of walkers converges to the absolute value of the wavefunction[10]; *not* $|\Phi|^2$. In the absence of importance sampling, the local energy is the potential energy. A plot of the 1-dimensional QHO with walker distribution is shown in Figure 9.

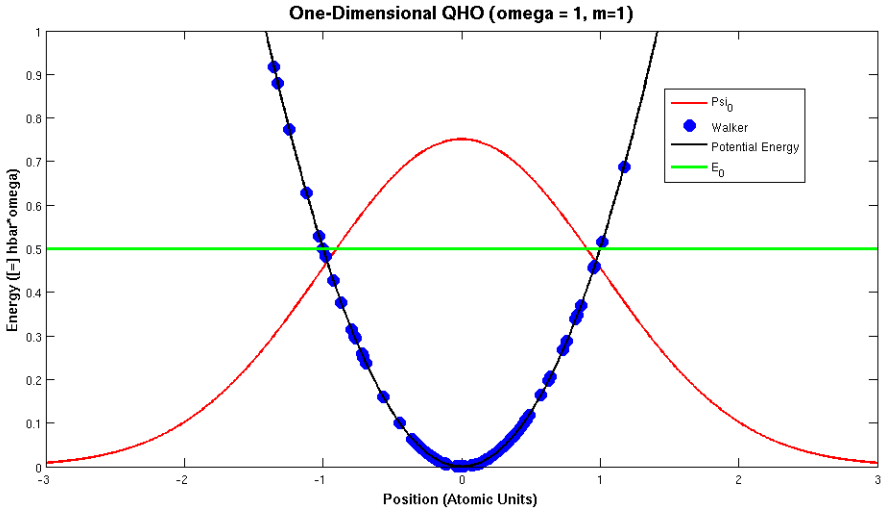

Figure 9: Walkers in a one-dimensional, unit width QHO.

As one can see, walker local energy (the potential energy at each walker's x-coordinate) averages to the ground-state energy, as predicted by the theorem in equation (21). In short, walkers are sample points used in statistical estimators for energy and wavefunction. Near the origin, local energy is less than the ground state energy, and the population density is greater. Farther out, in the classically forbidden region, where local energy is greater than the ground-state energy, walker population dwindles. If a walker diffuses toward the center of the well, then the energy of the system decreases. This has the greatest effect nearest to the center, where the most walkers are cloned. In the classically forbidden region, walkers will not be cloned. Although a walker is not cloned as it diffuses into the classically forbidden region, energy contributions increase quadratically, and are

[9] cf. [4, p. 256]
[10] cf. equation (21)

therefore non-negligible.

While our current $3N$-dimensional GFMC implementation thus far can compute ground state energies of certain quantum systems, much refinement is required before it can be used for more realistic cases. The biggest problem with our current implementation however is the exponential time and space complexity. As previously mentioned, a key point of Monte Carlo methods is to avoid this sort of computational complexity. Although aspects of our code work as we would like them to, until techniques are implemented to stabilize walker population, the code is useless for any sort of application. We shall therefore turn to the Diffusion Monte Carlo algorithm in an effort to obtain usable code, and figure out a solution to our walker growth problem in the process.

4 Diffusion Monte Carlo

Diffusion Monte Carlo (DMC) is another Monte Carlo algorithm which uses a similar walker implementation to that of GFMC. Incidentally, GFMC is a time-integrated version of DMC. We turn to DMC at this stage, because it is more widespread, and the extra documentation will make it easier to modify, debug, and refactor. Unlike GFMC, DMC does not use the exact time-independent Green's Function, but rather an approximation to the time-dependent Green's Function.

4.1 Overview

Given the $3N$-dimensional position vector $\mathbf{x}$, the time-dependent Schrödinger equation reads[11]

$$-\frac{\partial\Psi(\mathbf{x},t)}{i\partial t} = (\hat{H} - E_T)\Psi(\mathbf{x},t), \tag{32}$$

in units where $\hbar = 1$ and E_T is an energy shift. We may rewrite this equation in imaginary time ($\tau = it$) as follows:

$$-\frac{\partial\Psi(\mathbf{x},t)}{i\partial t} = -\frac{\partial\Psi(\mathbf{x},it)}{\partial it} = -\frac{\partial\Psi(\mathbf{x},\tau)}{\partial\tau} = [\hat{H} - E_T]\Psi(\mathbf{x},\tau). \tag{33}$$

Writing out the Hamiltonian and negating both sides, the equation becomes

[11] [7, p. 88]

$$\frac{\partial \Psi(\mathbf{x},\tau)}{\partial \tau} = D\nabla^2 \Psi(\mathbf{x},\tau) + (E_T - V(\mathbf{x}))\Psi(\mathbf{x},\tau), \tag{34}$$

where $D = \frac{\hbar^2}{2m} = \frac{1}{2}$ in atomic units[12] is the diffusion coefficient.

Ignoring the second term on the right hand side of the above equation yields

$$\frac{\partial \Psi(\mathbf{x},\tau)}{\partial \tau} = D\nabla^2 \Psi(\mathbf{x},\tau), \tag{35}$$

which is the $3N$-dimensional diffusion equation for which there exists an analytical solution. Likewise, ignoring the first term on the right hand side of the equation yields

$$\frac{\partial \Psi(\mathbf{x},\tau)}{\partial \tau} = (E_T - V(\mathbf{x}))\Psi(\mathbf{x},\tau), \tag{36}$$

which is a first order rate equation, whose solution may also be obtained analytically. Using the analytical solutions to equations (35) and (36), we may serially simulate these equations for many small discrete imaginary time steps to obtain an approximation of $\Psi(\mathbf{x},\tau)$.[13]

4.2 Time-Dependent Green's Function

We require an iterable solution to the ground state wavefunction. With the right Green's function, we may transform the imaginary time dependent Schrödinger equation to an integral equation of the form [14]

$$\Psi(\mathbf{y},\tau_2) = \int G(\mathbf{y},\tau_2;\mathbf{x},\tau_1)\Psi(\mathbf{x},\tau_1)dx. \tag{37}$$

Now, we can operate on both sides of equation (37) with $[\hat{H} - E_T]$ to obtain

$$[\hat{H} - E_T]\Psi(\mathbf{y},\tau_2) = \int [\hat{H} - E_T]G(\mathbf{y},\tau_2;\mathbf{x},\tau_1)\Psi(\mathbf{x},\tau_1)dx. \tag{38}$$

[12] This assumes equal particle masses, as we are dealing with in this paper. Unequal particle masses would require considering the sum of three-dimensional Laplacians acting on the position vector of each particle rather than one $3N-$dimensional Laplacian acting on the position vector of the configuration (in Cartesian coordinates). Several different D's would also be required for unequal masses.

[13] [7, p. 88]

[14] [7, p. 84]

We can also operate with $[-\frac{\partial}{\partial\tau_2}]$ to obtain

$$-\frac{\partial\Psi(\mathbf{y},\tau_2)}{\partial\tau_2} = \int -\frac{\partial G(\mathbf{y},\tau_2;\mathbf{x},\tau_1)}{\partial\tau_2}\Psi(\mathbf{x},\tau_1)dx. \tag{39}$$

Since equations (38) and (39) are equal by equation (33), we can equate their right hand sides[15]:

$$-\int \frac{\partial G(\mathbf{y},\tau_2;\mathbf{x},\tau_1)}{\partial\tau_2}\Psi(\mathbf{y},\tau_2)dx = \int[\hat{H}-E_T]G(\mathbf{y},\tau_2;\mathbf{x},\tau_1)\Psi(\mathbf{x},\tau_1)dx. \tag{40}$$

Simplification yields

$$-\frac{\partial G(\mathbf{y},\tau_2;\mathbf{x},\tau_1)}{\partial\tau_2} = [\hat{H}-E_T]G(\mathbf{y},\tau_2;\mathbf{x},\tau_1), \tag{41}$$

indicating that the Green's function satisfies the exact same form as the wavefunction. Solutions for both Green's function and wavefunction will be of the form [16]

$$\Psi(x,\tau) = \sum_{k=0}^{\infty} C_k\Phi_k(\mathbf{x})e^{-(E_k-E_0)\tau}, \tag{42}$$

and can also be expressed via the time evolution operator[17] as

$$|\Psi(\tau_2)\rangle = [e^{-(\hat{H}-E_\tau)(\tau_2-\tau_1)}]|\Psi(\tau_1)\rangle. \tag{43}$$

Operating with the unity operator $\mathbf{1} = \int d\mathbf{x}|\mathbf{x}\rangle\langle\mathbf{x}|$, multiplying by $\langle\mathbf{y}|$, and comparing to equation (39), we find that the Green's function can be expressed as the matrix element[18]

$$G(\mathbf{y},\tau_2;\mathbf{x},\tau_1) = \langle\mathbf{y}|e^{-(\hat{H}-E_\tau)(\tau_2-\tau_1)}|\mathbf{x}\rangle, \tag{44}$$

which incidentally depends only on the difference $\delta\tau = \tau_2 - \tau_1$. We now have an iterable integral equation of the form

$$\Psi(\mathbf{y},\tau+\delta\tau) = \int\langle\mathbf{y}|e^{-(\hat{H}-E_\tau)\delta\tau}|\mathbf{x}\rangle\Psi(\mathbf{x},\tau)d\mathbf{x}, \tag{45}$$

[15] [7, p. 84]
[16] [4, p. 23]
[17] [7, p. 85]
[18] [7, p. 86]

in which a stochastic matrix multiplies a state vector to produce a new state vector; similar to what we observed in GFMC. In this case, however, the Green's function represents the probability of a walker transitioning from state $\mathbf{x}$ to state $\mathbf{y}$ over the imaginary time step $\delta\tau$. By expanding the Green's function in eigenfunctions of the Hamiltonian, it can be shown that Ψ converges to the ground state wavefunction exponentially with the number of imaginary time steps taken.[19]

4.3 Implementation

Although we have the form of the integral equation from the previous section, obtaining an explicit representation of the time-dependent Green's function is generally not feasible. An approximation may be obtained by factoring the time evolution operator into kinetic and potential energy components:

$$e^{-(\hat{H}-E_\tau)(\delta\tau)} = e^{-(\hat{T}+V-E_\tau)(\delta\tau)} = e^{-\hat{T}\delta\tau}e^{(V-E_\tau)\delta\tau} + O(\delta\tau^2). \tag{46}$$

Error arising from the commutator of the kinetic and potential energy operators $\sim O(\delta\tau^2)$, so this approximation is valid only for $\delta\tau \ll 1$.[20] However, as $\delta\tau \to 0$, the approximation becomes the exact Green's function. We may write our Green's function approximation as

$$G \approx G_{Diff}G_{Branch} = e^{-\hat{T}\delta\tau}e^{(V-E_\tau)\delta\tau}, \tag{47}$$

where G_{Diff} is the Green's function corresponding to the solution of the diffusion equation and G_{Branch} is the Green's function corresponding to the solution of the rate equation.

The solution to the diffusion equation is[21]

$$\Psi = (4\pi D_\tau)^{-3N/2}e^{-(\mathbf{y}-\mathbf{x})^2/4D_\tau}, \tag{48}$$

and the solution to the branching equation is[22]

$$\Psi = e^{-(\frac{1}{2}(V(\mathbf{x})+V(\mathbf{y}))-E_T)\tau}, \tag{49}$$

[19] [7, pp. 86-87]
[20] [7, p. 89]
[21] [7, p. 89]
[22] [7, p. 89]

for small time $\tau = \delta\tau$.

By sampling from both distributions over a discrete time step, we are effectively iterating the integral equation. Now, the diffusion process is easy to simulate given a Gaussian random number generator. Perhaps the simplest technique is to sample from the one-dimensional solution for each coordinate of each walker and add the sampled value to the value of the coordinate.

The branching process is similar to that seen in GFMC: since we cannot have a fractional walker, the continuous probability density function in the branching solution must be converted to a probability mass function. Again, we may do this by flooring the result plus a uniform, random, double-precision floating point value on the interval $[0, 1]$. Thus, the probability mass function that we will sample from for the branching step is

$$MB = \text{int}(e^{-(\frac{1}{2}(V(\mathbf{x})+V(\mathbf{y}))-E_T)\delta\tau} + U[0, 1]), \tag{50}$$

Where $V(\mathbf{x})$ and $V(\mathbf{y})$ are the potential energy values for the walker before and after the diffusion step respectively. As before, $MB - 1$ copies of the walker are made. If $MB < 1$, $MB - 1$ walkers are removed from the ensemble.

4.4 Parameter Values, Ground-State Energy, and Convergence

Everything discussed vis-a-vis initialization for GFMC applies equally well to DMC. As previously stated, $\delta\tau$ should be at least an order of magnitude less than 1. We may interpret the walkers the same way as we did for GFMC as well: after enough iterations, a normalized bin of the walkers should yield the ground state wavefunction.

During preliminary tests of the DMC code for the one dimensional quantum harmonic oscillator potential, although the correct ground state wavefunction was obtained, problems of exponential walker growth occurred (which is the exact behavior we turned to DMC to try and mitigate). These walker growth problems were rectified by using a technique[23] in which trial energy is adjusted for each step so that the number of walkers remains more or less constant. The technique works as follows: the program starts out with a user defined number of walkers that we wish to maintain, which we shall denote N_{Target}. After the branching process for a given step, if $N > N_{target}$, we

[23]This technique and many parts of the working version of the code were adapted from [3].

increase the trial energy to remove walkers in the next iteration. Likewise, if $N < N_{Target}$, then we increase the trial energy so that more walkers are cloned in the next iteration. After enough iterations, the trial energy will converge to the ground-state energy. Another way to calculate ground-state energy besides taking the average of the local energies accross the ensemble is therefore to average the trial energy over many steps, once it converges to within uncertainty.[24] Although there are multiple ways to adjust the trial energy at each step, a common one is

$$E_T = E_T + \alpha\left(\frac{N_{Target}}{N}\right), \tag{51}$$

where $\alpha \ll 1$. This technique allows the trial energy to be written in good numerical form, where the new energy value is equal to the old value plus a small correction.[25] This technique fails, however, if initialization is way off (e.g. if $\delta\tau$ is too large), because too many walkers will be introduced or removed at each time step for meaningful results (or for internal memory in the extreme cases). This techniques is derived from the growth energy estimator[26], which offers an alternative method for finding ground state energy than averaging over the local energies of all walkers. We hypothesize that the technique illustrated in equation (51) will work for GFMC as well, but we have yet to implement it.

4.5 Preliminary Test Cases

To verify that our DMC code was working properly, we tested several quantum harmonic oscillator potentials, as we did for GFMC, and compared to the exact result. The table in Figure 10 shows a comparison of DMC code results for 1,2,3, and 4 particle QHO potentials with actual ground state energies ([=] $\hbar\omega$). Uncertainty was calculated as standard error. Averages were taken over 5000 steps, starting after 1000 steps. Target walker population was 10000 for 1,2, and 3 particle runs and 5000 for the 4 particle run. Initial trial energy was 0.0 for all runs.

One notices that the results obtained by the algorithm agree with the analytical solutions within uncertainty, indicating that the code is working properly. Moreover, walker population was kept

[24] As previously mentioned, this convergence is attained exponentially. For the systems we examine in this paper, convergence takes between $O(100)$ to $O(1000)$ steps.

[25] It does not particularly matter what mathematical form the correction factor takes, as long as it appropriately adjusts walker population and is small compared to E_T.

[26] cf. [7, p.99]

# Particles	DMC E_0	Error	Actual E_0
1	1.50	0.01	3/2
2	3.00	0.03	3
3	4.50	0.03	9/2
4	6.04	0.05	6

Figure 10: DMC results for 1,2,3, and 4 particle QHO potentials.

within a constant range. As expected, this range depends on $\delta\tau$, and the potential in question. Walker populations for two different values of $\delta\tau$ are shown in Figure 11.

Figure 11: Walker populations for the one-particle QHO with trial energy initialized at 0.0 and target walker population set to 10000. This target population is shown in black.

Incidentally, the size of the walker population range is directly related to the precision of results. As $\delta\tau \to 0$, the walker population becomes constant, and the short-time Green's function approximation becomes the exact Green's function.

Our code appears to be working for the QHO cases, but in order to be positive, we compared the normalized bin of the walkers to the normalization of the radial wavefunction for the one particle, three-dimensional QHO, which has form $R(r)_{norm} = Ce^{-r^2/2}$, where C is the normalization

constant.[27]

Since

$$C\int_0^\infty e^{-r^2/2}dr = C\frac{\sqrt{\pi}}{2} = 1, \tag{52}$$

the normalization constant is $\frac{2}{\sqrt{\pi}}$, and the normalization of the wavefunction is $R(r)_{norm} = \frac{2}{\sqrt{\pi}}e^{-r^2/2}$. Figure 12 contains a plot of the normalized bin of walkers as a function of radius. Walkers were binned and counted in a 500 element array, with bin spacing 0.01. The count was then normalized by dividing by the total number of walkers times the bin spacing. Results were obtained from a one particle 6000-step DMC run with step size 0.05 and 5000 as the target number of walkers. As expected, the normalized bin of the walker count with radius traces out $R(r)_{norm}$.

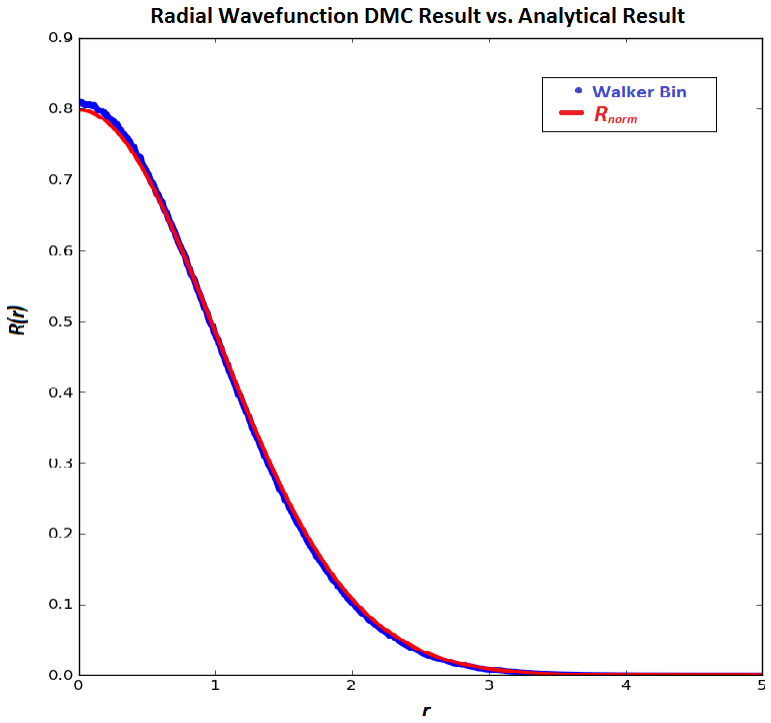

Figure 12: Normalized bin of DMC walkers and actual wavefunction for the 1-particle QHO.

[27] cf. Section 5.2

5 Implementing Particle Interactions

Now that we have tested the code for the several particle QHO potential, we wish to implement realistic[28] pairwise boson interactions of the form

$$V = \sum_{i=1}^{N} \sum_{j<i} V_0 e^{-|r_i - r_j|^2/r_0^2}, \tag{53}$$

for a system of N particles confined in a harmonic trap.

As previously stated, the raison d'être of quantum numerical solutions is that the Schrödinger equation for realistic systems generally has no exact analytical solution, and the harmonically confined boson system is no exception. This presents the problem of verifying whether or not our implementation of the DMC algorithm is working as it should, once we implement these interactions.

Auspiciously, an analytical approximation of the ground state energy for low-energy interactions is feasible via first-order perturbation theory. We shall devote the remainder of this section to obtaining this approximation and compare the result to the output from our DMC program.

5.1 First-Order Perturbation Theory

Time-independent perturbation theory yields an approximation to the ground state energy for a system that is similar to a system for which an exact analytical solution is known. In our case, there exists an analytical solution to the N-particle quantum harmonic oscillator, the unperturbed configuration, and we wish to obtain an approximation to the ground state energy of an N-particle system, harmonically bound with pairwise Gaussian interactions of the form $V_0 e^{-|r_i - r_j|^2/r_0^2}$. If the energy contributions from the particle interactions are small ($V_0 \ll \hbar\omega$), then we can apply first-order perturbation theory to obtain a solution to within DMC uncertainty.

The idea of perturbation theory is to write out the Hamiltonian operator of the perturbed configuration in terms of the Hamiltonian operator of the unperturbed configuration plus a small correction, so that

$$H = H^0 + \lambda H', \tag{54}$$

where H^0 is the unperturbed Hamiltonian operator, H is the perturbed Hamiltonian operator, λ

[28] [9]

is constant, and H' is the Hamiltonian operator of the perturbation (cf. [4, pp.221-223]). By expanding the ground state wavefunction and energy of the new Hamiltonian operator as a power series in λ about the corresponding wavefunction and energy values for the unperturbed Hamiltonian operator, we can write the the Schrödinger equation for the perturbed system as

$$(H^0 + \lambda H')\psi^{new}{}_0 = E^{new}\psi^{new}{}_0, \tag{55}$$

with ψ^{new} and E^{new} expressed as power series. By power matching, we can set first-order λ coefficients on the left hand side of the equation equal to first-order λ coefficients on the right hand side of the equation. Taking the inner product with $\langle\psi^0{}_0|$ and recognizing orthonormality leaves us with the result that

$$E_0{}^1 = \langle\psi^0{}_0|H'|\psi^0{}_0\rangle, \tag{56}$$

where $E_0{}^1$ is the first-order energy correction. In our case, H' will simply be the change, $\sum_{i=1}^{N}\sum_{j<i} V_0 e^{-\frac{|\vec{r}_j-\vec{r}_i|^2}{{r_0}^2}}$, to the potential energy of the system due to particle interactions. Hence, given the N-particle QHO ground state wavefunction, Ψ_0, the ground state energy of the confined system will be changed by

$$\Delta E = \langle\Psi_0|\sum_{i=1}^{N}\sum_{j<i} V_0 e^{-\frac{|\vec{r}_j-\vec{r}_i|^2}{{r_0}^2}}|\Psi_0\rangle \tag{57}$$

when Gaussian interactions are accounted for.

5.2 Jacobi Coordinates

The expression in equation (57) for the change in energy due to pairwise particle interactions, though straightforward to obtain is somewhat cumbersome to evaluate, since it involves a $3N$-dimensional Gaussian integral. Although there may be multiple methods for attacking this monster, the method we will use involves a transformation to Jacobi coordinates. Therefore, a brief discussion of these coordinates is in order.

The term "Jacobi coordinates" actually refers to several different coordinate systems. We are interested in K-type Jacobi coordinates (cf. [12, pp.36-38]), which are constructed iteratively. The first Jacobi vector, $\vec{\rho}_1$ points from the center of mass of particle 1 to the center of mass of particle

2. The second Jacobi vector, $\vec{\rho}_2$ points from the center of mass of particles 1 and 2 to the center of mass of particle 3. The third Jacobi vector, $\vec{\rho}_3$, points from the center of mass of particles 1,2, and 3 to the center of mass of particle 4, and so on. There is also a center of mass vector from the origin of the Cartesian coordinate system to the center of mass of all N particles. Thus, for a 4-particle system, a K-type Jacobi coordinate scheme would be[29]

$$\vec{\rho}_1 = \vec{r}_1 - \vec{r}_2 \tag{58}$$

$$\vec{\rho}_2 = \frac{m_1\vec{r}_1 + m_2\vec{r}_2}{m_1 + m_2} - \vec{r}_3 \tag{59}$$

$$\vec{\rho}_3 = \frac{m_1\vec{r}_3 + m_2\vec{r}_2 + m_3\vec{r}_3}{m_1 + m_2 + m_3} - \vec{r}_4 \tag{60}$$

$$\vec{X}_{cm} = \frac{m_1\vec{r}_3 + m_2\vec{r}_2 + m_3\vec{r}_3 + m_4\vec{r}_4}{m_1 + m_2 + m_3 + m_4}, \tag{61}$$

and is illustrated in Figure 13.

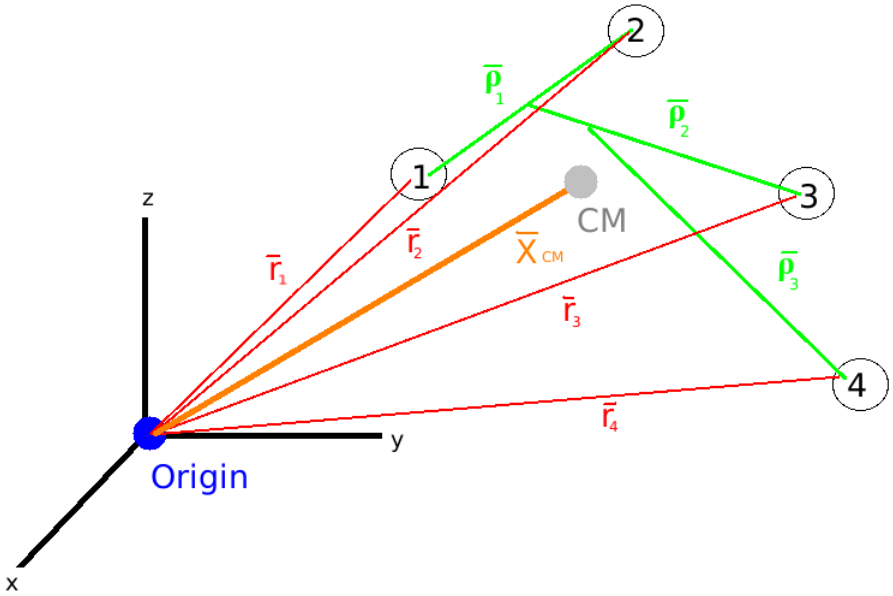

Figure 13: The K-type Jacobi coordinate system in equations (58)-(61). Notice the K-shape of the Jacobi vectors (shown in green).

Jacobi coordinates are convenient when dealing with spherically symmetric potentials, because solutions are separable into relative and center-of-mass terms (cf. [9]). Moreover, if an isotropic

[29][12, pp.36-38]

change is introduced to the potential (e.g. Gaussian particle interactions) it will not affect the center of mass solution and only the relative equation need be considered.

5.3 2-Particle Perturbation Theory Solution

We first consider the solution to the two-particle system, as it will be readily generalizable to the N-particle system. Applying first-order perturbation theory indicates that the change in energy due to the particle interactions will be

$$\begin{aligned}\Delta E &= \langle \Psi_0 | V_{1,2} | \Psi_0 \rangle \\ &= V_0 \int_{\mathbf{D}} e^{-({x_1}^2+{y_1}^2+{z_1}^2+{x_2}^2+{y_2}^2+{z_2}^2)} e^{-((x_1-x_2)^2+(y_1-y_2)^2+(z_1-z_2)^2)/{r_0}^2} dx_1 dy_1 dz_1 dx_2 dy_2 dz_2,\end{aligned} \tag{62}$$

a six-dimensional integral, with integration domain ($\mathbf{D}$) ranging from $-\infty$ to ∞ over all six Cartesian coordinates. Evaluation appears impossible at first (Try it!). While this integral could be evaluated numerically via composite Simpson integration or Gaussian quadrature, we may obtain an exact analytical solution by separating the Hamiltonian into center of mass and relative components and considering only the relative wavefunction.[30] Although this technique will produce an apparently different matrix element, separation of variables guarantees that it will evaluate to the same result as the integral in equation (62). Hence, we may write

$$\Delta E = \langle \psi_{0rel} | V_{12} | \psi_{0rel} \rangle, \tag{63}$$

where ψ_{0rel} is the relative ground-state wavefunction for the 6-dimensional quantum harmonic oscillator, and $V_{12} = V_0 e^{-\frac{|\vec{r}_1 - \vec{r}_2|^2}{{r_0}^2}}$.

We now introduce a transformation to Jacobi coordinates where

$$\vec{\rho} = \vec{r}_1 - \vec{r}_2 \tag{64}$$

and

[30] This may be done because isotropic pairwise interactions have no effect on the center of mass behavior of the system (cf. [9]).

$$\vec{X}_{cm} = \frac{m_1\vec{r}_1 + m_2\vec{r}_2}{m_1 + m_2}. \tag{65}$$

The relative Schrödinger equation becomes[31]

$$\left[-\frac{\hbar^2}{2\mu}{\nabla_\rho}^2 + \frac{1}{2}\mu\omega|\vec{\rho}|^2\right]\psi_{rel} = E\psi_{rel}, \tag{66}$$

where $\mu = \frac{m_1 m_2}{m_1+m_2}$ is the reduced mass of both particles. Because we are dealing with an isotropic potential, we are guaranteed separable solutions for both magnitude and directional components of $\vec{\rho}$. Hence, it is convenient to adopt spherical coordinates, where

$$\psi_{0rel} = \psi_{0rel}(\rho, \theta, \phi) = R(\rho)Y(\theta, \phi). \tag{67}$$

The spherical harmonics in this case are the same as for the hydrogen atom[32]:

$$Y(\theta, \phi) = \sqrt{\frac{1}{4\pi}}. \tag{68}$$

Therefore, all that remains for us to do is to solve for $R(\rho)$. Note that we need only consider the ρ terms of the spherical Laplace operator in the radial equation, which becomes

$$\left[-\frac{\hbar^2}{2\mu}\frac{1}{\rho^2}\frac{d}{d\rho}\left(\rho^2\frac{d}{d\rho}\right) + \frac{1}{2}\mu\omega\rho^2\right]R = ER. \tag{69}$$

Making the change of variables $u(\rho) = R(\rho)/\rho$, causes the equation to become

$$\left[-\frac{\hbar^2}{2\mu}\frac{d^2}{d\rho} + \frac{1}{2}\mu\omega\rho^2\right]u = Eu, \tag{70}$$

which is simply the one-dimensional quantum harmonic oscillator time-independent Schrödinger equation with different boundary conditions. Specifically, these boundary conditions are necessary to keep R normalizable. Normalization requires that $u \to 0$ as $\rho \to \infty$ and $u \to 0$ as $\rho \to 0$. We know, from the standard power-series solution to the one-dimensional QHO equation, that the first solution which accommodates this boundary behavior corresponds to the first odd coefficient of the

[31] [9]

[32] cf. [4, p.128]

power series (cf.[4, pp.37-41]). Thus, the solution to the u equation will be the first excited state solution to the one-dimensional quantum harmonic oscillator with a different normalization range. For the one-dimensional QHO case, the limits on x for the normalization integral went from $-\infty$ to ∞. For the u equation, however, the limits on ρ go from 0 to ∞. Hence, normalization demands that

$$\int_0^\infty u^* u d\rho = \int_{-\infty}^\infty {\psi_{1D}}^* \psi_{1D} dx = 1. \tag{71}$$

Since u is real u^*u is simply equal to u^2. By symmetry, the normalized u solution is $\sqrt{2}$ times the normalized first excited state solution to the one-dimensional QHO equation, and reads[33]

$$u = 2\left(\frac{\mu\omega}{\pi\hbar}\right)^{\frac{1}{4}} \sqrt{\frac{\mu\omega}{\hbar}} \rho e^{-(\frac{\mu\omega}{\hbar}\rho^2)/2}. \tag{72}$$

Dividing by ρ,

$$R = 2\left(\frac{1}{\pi}\right)^{\frac{1}{4}} \left(\frac{\mu\omega}{\hbar}\right)^{\frac{3}{4}} e^{-(\frac{\mu\omega}{\hbar}\rho^2)/2}, \tag{73}$$

and the relative ground state wavefunction becomes

$$\psi_{0rel} = R(\rho)Y(\theta,\phi) = \left(\frac{1}{\pi}\right)^{\frac{3}{4}} \left(\frac{\mu\omega}{\hbar}\right)^{\frac{3}{4}} e^{-(\frac{\mu\omega}{\hbar}\rho^2)/2}. \tag{74}$$

An inner product will confirm that this solution is normalized. While the relative ground state energy is not necessary for our perturbation theory solution, since we only care about *change* in energy, it is worth noting that $E_{0_{rel}} = \frac{3}{2}\hbar\omega$.

Now that we have the relative wavefunction, we can obtain the energy change due to the perturbation. Since we are currently concerned with particles of unit mass in a unit width well (in atomic units), we may replace $\hbar$ and ω in equation (74) with 1, and the reduced mass factor (μ) with $\frac{1}{2}$. The inner product becomes

$$\Delta E = \langle\psi_{0rel}|V_{1,2}|\psi_{0rel}\rangle = V_0 \int_0^{2\pi}\int_0^{\pi}\int_0^{\infty} \rho^2 \left(\frac{1}{2}\right)^{\frac{3}{2}} \left(\frac{1}{\pi}\right)^{\frac{3}{2}} e^{-\frac{\rho^2}{2}} e^{-\frac{\rho^2}{{r_0}^2}} \sin\theta d\rho d\theta d\phi. \tag{75}$$

An evaluation of the angular coordinates yields

[33] cf. [4, 41]

$$\Delta E = \langle \psi_{0rel} | V_{1,2} | \psi_{0rel} \rangle = 4\pi V_0 \left(\frac{1}{2}\right)\left(\frac{1}{\pi}\right)^{\frac{3}{2}} \int_0^\infty \rho^2 e^{-\rho^2(\frac{1}{2}+\frac{1}{{r_0}^2})} d\rho, \tag{76}$$

which evaluates analytically to

$$\Delta E(V_0) = \frac{V_0}{(1+\frac{2}{{r_0}^2})^{\frac{3}{2}}}. \tag{77}$$

This result can be confirmed numerically for several r_0 values by partitioning the integral in equation (62) into the product of three double-integrals times V_0 (one integral for each Cartesian coordinate pair). Since each double integral evaluates to the same result, this is equivalent to multiplying V_0 by the the cube of the result of one double integral. The double-integral can be evaluated by transforming to polar coordinates, evaluating the angular portion analytically, then evaluating the radial portion via composite Simpson $\frac{3}{8}$ integration. If our DMC code is working properly, we expect a plot of ground-state energy vs. V_0 obtained from the program to have the same slope as the perturbation result for a fixed r_0 value.

5.4 N-Particle Perturbation Theory Solution

We now generalize our perturbation-theory solution to the N-particle case, where the change in energy due to the perturbation is the matrix element

$$\begin{aligned} \Delta E &= \langle \Psi_0 | \sum_{i=1}^{N} \sum_{j<i} V_0 e^{-\frac{|\vec{r}_i - \vec{r}_j|^2}{{r_0}^2}} | \Psi_0 \rangle \\ &= \int_{\mathbf{D}} \sum_{i=1}^{N} \sum_{j<i} V_0 e^{-\frac{|\vec{r}_i - \vec{r}_j|^2}{{r_0}^2}} e^{-({x_1}^2+{y_1}^2+{z_1}^2+\ldots+{x_N}^2+{y_N}^2+{z_N}^2)} dx_1 dy_1 dz_1 \ldots dx_N dy_N dz_N, \end{aligned} \tag{78}$$

a $3N$-dimensional integral, with integration domain ($\mathbf{D}$) ranging from $-\infty$ to ∞ over all $3N$ Cartesian coordinates. The result of this integral is equal to the $3(N-1)$-dimensional integral

$$\Delta E = \langle \psi_{0rel} | V_0 \sum_k e^{-\frac{{\rho_i}^2}{{r_0}^2}} | \psi_{0rel} \rangle = V_0 \int_0^\infty \ldots \int_0^\infty \sum_k e^{-\frac{{\rho_i}^2}{{r_0}^2}} (\psi_{0rel}(\rho))^2 d^3\rho_1 \ldots d^3\rho_{(N-1)} \tag{79}$$

in Jacobi coordinates, where k corresponds to the ith and jth particle indices in Cartesian coordinates. Now, we wish to obtain ψ_{0rel}. Since the D-dimensional quantum harmonic oscillator is separable into D one-dimensional quantum harmonic oscillators, and each harmonic oscillator's solution is separable into relative and center-of-mass components, the relative $3(N-1)$ dimensional Jacobi coordinate wavefunction is separable into $N-1$ three-dimensional Jacobi coordinate wavefunctions. We found the three-dimensional Jacobi coordinate wavefunction to be

$$\psi_{0rel} = R(\rho)Y(\theta,\phi) = \left(\frac{1}{\pi}\right)^{\frac{3}{4}}\left(\frac{\mu\omega}{\hbar}\right)^{\frac{3}{4}} e^{-(\frac{\mu\omega}{\hbar}\rho^2)/2}, \tag{80}$$

in section 5.3. By separation of variables, the $3(N-1)$-dimensional wavefunction is

$$\psi_{0rel} = \left(\frac{1}{\pi}\right)^{\frac{3(N-1)}{4}}\left(\frac{\mu\omega}{\hbar}\right)^{\frac{3(N-1)}{4}} e^{-(\frac{\mu\omega}{\hbar}({\rho_1}^2+{\rho_2}^2+\ldots+{\rho_{(N-1)}}^2)/2}, \tag{81}$$

where $\vec{\rho_i} = \vec{r_i} - \vec{r_j}; j < i$. Note that we are exploiting isotropic symmetry by treating each particle-pair with a different K-type Jacobi coordinate scheme. Because there is no quantitative distinction between each Jacobi coordinate in equation (81), the inner product $\langle\psi_{0rel}|\sum_k e^{-\frac{{\rho_i}^2}{{r_0}^2}}|\psi_{0rel}\rangle$ is equivalent to $\sum_k\langle\psi_{0rel}|V_0 e^{-\frac{{\rho_i}^2}{{r_0}^2}}|\psi_{0rel}\rangle$. Now, for each element of the sum, the components terms of ψ_{0rel} that do not involve ρ_i effectively become one, allowing the inner product to be written as the sum of two-particle perturbations,

$$\Delta E = \sum_k \frac{V_0}{(1+\frac{2}{{r_0}^2})^{\frac{3}{2}}}. \tag{82}$$

Now all that remains is to figure out the range of the k-index. For this, we use elementary combinatorics. Since we are considering the total number of particle pair interactions, without replacement, without regard to order, the sum will range from 1 to $\binom{N}{2}$ for N-particles. Therefore, the change in energy as a result of the aforementioned Gaussian particle interactions can be approximated as

$$\Delta E = \binom{N}{2}\frac{V_0}{(1+\frac{2}{{r_0}^2})^{\frac{3}{2}}} = \frac{V_0 N(N-1)}{2(1+\frac{2}{{r_0}^2})^{\frac{3}{2}}} \tag{83}$$

for the N-particle system.

5.5 Comparison of First-Order Perturbation Theory Approximation with DMC Results

The plots in Figure 14 contain comparisons of ground state energies obtained via DMC and first-order perturbation theory approximations. In the perturbative regime, where the magnitude of the perturbation is no greater than an order of magnitude less than the ground state energy, the results agree to within DMC uncertainty, with an osculation point at $V_0 = 0$.

As the magnitude of V_0 increases, higher-order terms in the power series become non-negligible and the linear extrapolation becomes progressively worse. This is exactly the physical behavior that we would expect, indicating that the DMC code is working properly for bosons with pairwise Gaussian interactions in a harmonic trap. Additionally, rate of deviation from the first-order result for constant V_0 increases as $O(N^2)$ as additional particles are added,[34] as we would also expect, since more particles confined to the same volume result in a higher magnitude relative energy system, depending on the whether the attractions are attractive or repulsive.[35]

[34] cf. equation (83)

[35] This alludes to the concept of quantum pressure.

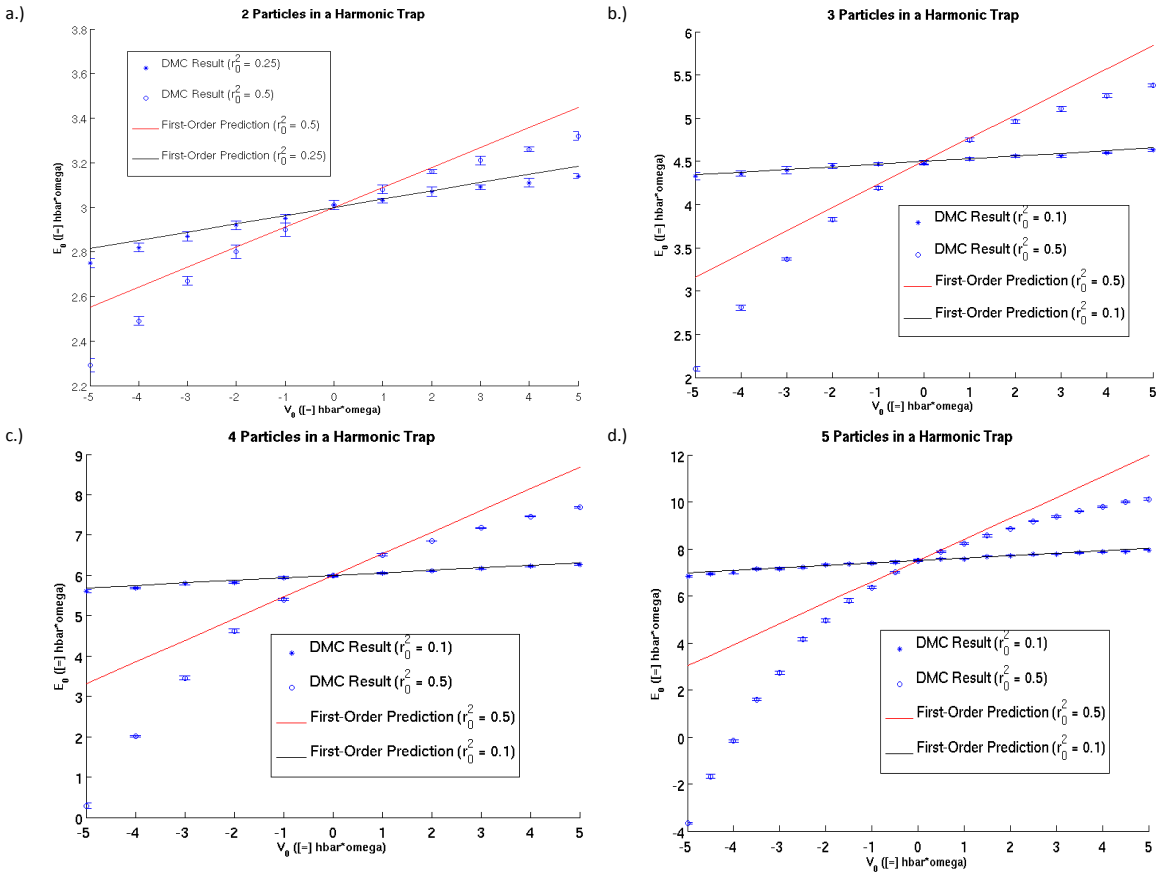

Figure 14: DMC results and first-order perturbation theory predictions for harmonically confined bosons with pairwise Gaussian interactions.

6 Conclusion

We have presented two Monte Carlo Algorithms which can be used to compute the ground state energies of bound quantum multi-particle systems. Both GFMC and DMC algorithms have their inherent advantages and disadvantages. GFMC has the advantage that it uses an exact Green's function and is therefore more accurate. A key tradeoff, however, which perhaps accounts for the widespread favortism of DMC is that GFMC requires esoteric probability density function transformations, which are error-prone and time-consuming to implement, especially in the low-level compiled languages (e.g. C++ or Fortran) necessary for runtime considerations.

An implementation of the Green's Function Monte Carlo algorithm was used to correctly compute the ground state energies of the $3N$-dimensional quantum harmonic oscillator. Although the problem of walker growth for this algorithm has not yet been corrected, the solution utilized for DMC of changing the trial energy should work equally well in GFMC. The Diffusion Monte Carlo algorithm was used to compute the ground state energies for realistic harmonically confined systems of bosons with pairwise Gaussian interactions, for which there exist no analytical solutions. The veracity of this DMC approximation was verified via a first-order perturbation approximation.

With little extension, this DMC code may be used to model condensed matter problems with tens, or perhaps hundreds of particles in polynomial time, which cannot be done with traditional techniques such as matrix diagonalization, or finite-difference mesh methods, which go as $O(e^N)$.[36] Since exponential time complexity is not resolvable, irrespective of technological advances, Monte Carlo algorithms have and will continue to have a necessary role in many-particle quantum mechanics.

[36]The specific time complexity on the DMC problem for Gaussian particles in a harmonic trap is $O(N^2)$, which is a consequence of pairwise interactions and can be seen in the N-particle perturbation theory approximation.

References

[1] J.B. Anderson, J. Chem. Phys. 86, 2839 (1986).

[2] R.L. Burden and J.D. Faires,*Numerical Analysis* (Brookes/Cole, Cengage Learning, Boston MA, 2011).

[3] Computational Physics 411-506. University At Buffalo, 15 Apr. 2004. Web. 17 Jan. 2012. <http://www.physics.buffalo.edu/phy411-506-2004/lectures.html>

[4] D.J. Griffiths, *Introduction to Quantum Mechanics* (Prentice-Hall, Upper Saddle River NJ, 1994).

[5] R. Guardiola, *Monte Carlo Techniques in the Many Body Problem* (1988 Unpublished Notes).

[6] K. Gottfried and T. Yan, *Quantum Mechanics: Fundamentals 2nd Edition*, (Springer-Verlag, New York NY, 2004).

[7] B.L. Hammond, W.A. Lester and P.J. Reynolds, *Monte Carlo Methods in Ab Initio Quantum Chemistry* (World Scientific, Singapore, 1994).

[8] M.H. Kalos, Physical Review A 128, 1791 (1962).

[9] W. Krauth, Physical Review Letters 77 3695 (1996).

[10] N. Metropolis et al., J. Chem. Phys. 21, 1087 (1953).

[11] P. Olofsson, *Probability, Statistics, and Stochastic Processes* (Wiley-Interscience, Hoboken NJ, 2005).

[12] S.T. Rittenhouse et al., J. Phys. B. 44, 172001 (2011).